Research Article

Modeling, simulation and experimental exploration of metal magnetic memory under weak magnetic excitation

Bo Liu[1,3] · Juwei Zhang[2,3] · Zengguang Zhang[2,3]

Abstract

This study proposes to use the improved Jiles–Atherton (J–A) magneto-mechanical effect model combined with simulation analysis to detect the damage of wire rope. By establishing the theoretical basis of the J–A model under weak magnetic excitation, the simulation analysis is carried out by using ANSYS software, and finally the correctness of the simulation and theoretical results is verified by experiments. The results show that the weak magnetic excitation magnetic field has a strengthening effect on the magnetic memory signal under the action of the force-magnetic coupling. By processing the extracted magnetic memory signal, it is verified that the weak magnetic excitation magnetic field alone has a certain inhibitory effect on the environmental interference of the geomagnetic field. Compared with the geomagnetic field environment, the weak magnetic excitation magnetic field can better identify the different defect types of simulated 60 steel damage and wire rope defects. Studies have shown that weak magnetic excitation plays an important role in the damage detection of ferromagnetic materials.

Article highlights

1. Improve and establish the theoretical model of J–A magneto-mechanical effect under weak magnetic excitation.
2. Magnetic memory signal can distinguish different damage types, and weak magnetic excitation can strengthen magnetic memory signal.
3. Force-magnetic coupling experiment verifies the effectiveness of weak magnetic excitation field in defect identification.

Keywords Metal magnetic memory · Weak magnetic excitation · ANSYS modeling and simulation · Force-magnetic coupling · Strengthening

1 Introduction

In modern industrial fields, industrial products are increasingly developing in the direction of high speed, high temperature, and high load. Fatigue damage has become a prominent problem in various industrial sectors. Therefore, the analysis of fatigue damage and the effective evaluation of stress and deformation have become an important basis for evaluating the structural strength and reliability of equipment and components. For the detection of micro-defects caused by stress concentration [1], it is of great significance to prevent the early failure of ferromagnetic specimens [2, 3]. In the late 1990s, Russian scholars represented by Professor Dubov took the lead in proposing a new non-destructive testing technology-metal magnetic memory testing [4]. The basic principle is that when the working load and the geomagnetic field act together, the magnetic properties of the materials will change due to the force-magnetic coupling effect [5], so that the location of material defects and stress concentration and the degree of damage can be determined by measuring the spontaneous magnetic field signal formed on the surface of the test piece [6], and the metal magnetic memory detection technology has more advantages in monitoring the stress and strain state of complex material structures [7]. However, the environmental magnetic field based on the terrestrial magnetic field is a relatively weak magnetic field, which is easily affected by the chemical composition and defect shape of the ferromagnetic material itself, and the change characteristics of the magnetic memory signal are easily affected [8]. [9] shows that the reason for the different results of the magnetic memory test may be that the weak magnetic signal is very susceptible to the interference of the environmental magnetic field, and it is difficult to obtain effective results. [10] explores to improve the sensitivity and reliability of magnetic memory detection by using the enhanced magnetic excitation field, but the influence of the geomagnetic field environment cannot be ruled out.

At present, the magnetic memory testing of the test piece in the metal magnetic memory testing technology is mainly based on the influence of various factors such as temperature, defect shape and different materials on the change of the magnetic memory signal [11], and through its normal component and cut to determine the stress concentration location based on the curve characteristics of the directional component. [12, 13] explore the influence of the environmental magnetic field on the magnetic memory signal of each point of the test piece from the experimental point of view. The mechanism of magnetic memory is an important part of the study of changes in magnetic memory signals. [14] explores and extracts the components of the magnetic memory normal and tangential signals at the stress concentration of the test piece, and compares the average value and its gradient value to determine the stress concentration area from the appearance characteristics of the magnetic memory signal. [15] explores the relationship between normal and tangential magnetic memory signals and different factors such as lift-off value, defect depth, width and so on from a macro perspective. Research shows that each factor has varying degrees of influence on magnetic memory signal, In summary, exploring the mechanism of magnetic memory and the change characteristics of magnetic memory signals at defects or stress concentration areas under weak magnetic excitation will be more conducive to distinguish the damage of the specimen.

In the second part of this paper, from the perspective of combining microscopic and macroscopic, based on the J–A force-magnetic coupling model, combined with the relationship between stress, permeability and environmental magnetic field, the influence of external weak magnetic excitation magnetic field on magnetic field factors is theoretically discussed. The third part analyzes the change of the magnetic memory signal under different loading conditions, the geomagnetic field and the weak magnetic excitation magnetic field environment on the basis of the force-magnetic coupling theory by ANSYS simulation. The changes of the magnetic memory signal in the environmental magnetic field of different intensities were analyzed under the condition of eliminating the influence of the geomagnetic field on the magnetic memory signal, and the characteristics of the magnetic memory signal of the specimen under the action of a single weak magnetic excitation magnetic field were explored. The fourth part of this paper analyzes and verifies the effect of weak magnetic excitation through actual experiments, and reveals the effectiveness of weak magnetic excitation for damage detection of protruding wire ropes.

2 Theoretical analysis

2.1 Improved Jiles–Atherton model

When the polycrystalline bulk ferromagnetic material is subjected to uniaxial stress, the magnetization formed under the action of an external magnetic field includes reversible magnetization caused by domain wall bending and irreversible magnetization caused by domain wall displacement and magnetic domain rotation, among which the external magnetic field Energy, demagnetization energy, and magnetoelastic energy have a greater impact on the

magnetization process [16]. According to the law of thermodynamics, when the ferromagnetic material is placed in an external magnetic field and subjected to a tensile load and the stress is coaxial with the magnetic field [17], the total internal energy satisfies:

$$A = \mu_0 HM + \frac{\mu_0}{2}\alpha M^2 + \frac{3}{2}\sigma\lambda + TS \tag{1}$$

where μ_0 is the vacuum permeability, H is the external magnetic field, α is the Weiss molecular field coefficient, which describes the coupling relationship between the magnetic domains in the material, T is the temperature, S is the entropy, λ is the magnetostriction coefficient, and M is Magnetization.

In the geomagnetic field environment, under the action of the ferromagnetic body under stress, the discontinuous parts inside the material will produce uneven distribution of stress, which will cause the strain with magnetostrictive properties, and the phenomenon of stress concentration will occur. Under the action of stress, the magnetic domains and domain walls will undergo irreversible movement, resulting in stress energy, which in turn will form magnetic poles, and generate a leakage magnetic field on the surface of the component, forming a magnetic memory effect.

The proximity principle shows that under the action of stress, the remanent magnetization state of ferromagnetic materials will irreversibly and infinitely approach the hysteresis-free magnetization state [18], and based on the effective field theory, the unidirectional stress state of iron is established under the elastic stress state. Magneto-mechanical model of magnetic materials-Jiles–Atherton theoretical model [19]. The J–A model equates the action of stress as an equivalent magnetic field in the same direction as the stress, that is, the applied stress changes the internal effective field through the influence on the magnetostriction coefficient, which is equivalent to adding an equivalent magnetic field H_σ. Then through the derivation of the magnetization model, the force-magnetic coupling model can be obtained, and then the influence of stress on the magnetization can be quantified. The J–A theoretical model explains the relationship between stress and non-hysteresis magnetization, between stress and stress equivalent field, and between stress and magnetization in the form of a first-order differential equation. The relationship is as follows:

$$M_{an}(H, \sigma) = M_s\left[\coth\left(\frac{H_{eff}}{a}\right) - \frac{a}{H_{eff}}\right] \tag{2}$$

$$H_\sigma = \frac{3\sigma}{\mu_0}\left[(\gamma_1 + \gamma_1'\sigma)M_{an} + 2(\gamma_2 + \gamma_2'\sigma)M_{an}^3\right] \tag{3}$$

$$H_{eff} = \frac{1}{\mu_0}\frac{dA}{dM} = H + H_\sigma + \alpha M_{an} \tag{4}$$

where H_σ is the stress equivalent field, M_{an} is the non-hysteresis magnetization, γ_1, γ_1', γ_2, γ_2' are the magnetostrictive parameters, σ is the stress, and M_s is the saturation magnetization.

When considering the geomagnetic field as the main external excitation magnetic field, the strength of the magnetic field is relatively weak and it is susceptible to interference from external factors, and different external magnetic fields will produce different magnetization. Based on the fact that the greater the magnetization, the greater the stress equivalent field. And the larger the magnetic memory signal, the external magnetic field term with weak magnetic excitation—H_W is added to Eq. (4), and the improved equivalent magnetic field formula is as follows:

$$H_{eff} = \frac{1}{\mu_0}\frac{dA}{dM} = H + H_w + H_\sigma + \alpha M_{an} \tag{5}$$

Based on the above-mentioned magnetomechanical effect theory, through the research results of Kuruzar and Cullity [20], combined with the analysis of the influence of magneto-mechanical effect model parameters on stress magnetization curve [21], the numerical simulation of the force-magnetic coupling effect of the specimen is carried out, and the parameters are selected as follows: $\alpha = 1 \times 10^{-3}$ A/m, a $= 1 \times 10^3$ A/m, c $= 0.1$, E $= 217 \times 10^9$ Pa, $\xi = 2000$ Pa, $\gamma_1 = 10^{-18}$, $\gamma_1' = -2 \times 10^{-26}$, $\gamma_2 = 2 \times 10^{-30}$, $\gamma_2' = -5 \times 10^{-38}$, through Eq. (2) is calculated by Matlab numerical simulation, and the equivalent magnetic field intensity under different external magnetic field excitation can be obtained with the change of stress. As shown in Fig. 1.
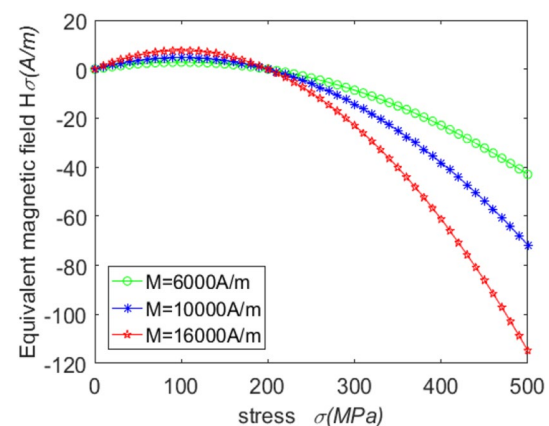

Fig. 1 Variation curves of stress and equivalent stress field

$$\frac{dM_{an}}{d\sigma} = \frac{dM_{an}}{dH_{eff}} \frac{dH_{eff}}{d\sigma} \tag{6}$$

Equation (6) represents the change of non-hysteresis magnetization with stress. From the relationship of Eq. (6), it can be seen that the non-hysteresis magnetization does not always increase with the increasing stress. Under the geomagnetic field, after the stress reaches 100 MPa, the non-hysteresis magnetization decreases with the increase of the stress. With the continuous increase of the applied magnetic field intensity, the trend of non-hysteresis magnetization gradually decreases.

$$\frac{dM}{d\sigma} = \frac{\sigma}{E\zeta}(M_{an} - M) + c\frac{dM_{an}}{d\sigma} \tag{7}$$

The first-order differential equation shown in Eq. (7) is a function of the change of magnetization with stress. In the geomagnetic field environment, as the tensile stress increases, the magnetization first increases, and after the stress reaches 100 MPa, the magnetization gradually decreases. After applying a weak magnetic field excitation, with the continuous increase of the external weak magnetic excitation magnetic field, the magnetization increases with the increase of the stress, but the stress value corresponding to the peak value gradually decreases as shown in Fig. 2

With the increase of the external weak magnetic excitation magnetic field, the magnetization in the ferromagnet continues to increase. As the external magnetic field continues to increase in the stress concentration area of the ferromagnet, the leakage magnetic field generated in the stress concentration area will be excited by the external weak magnetic field. If it becomes larger, the magnetic
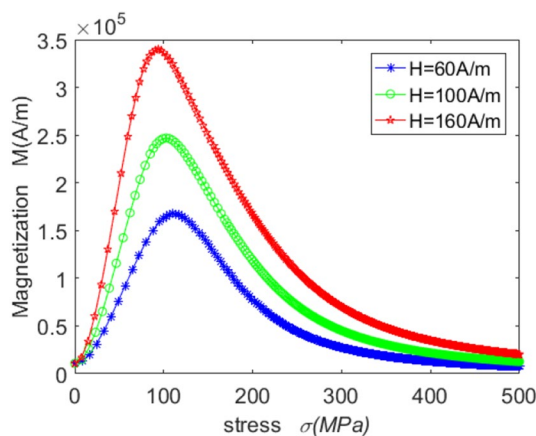

Fig. 2 Variation curves of magnetization intensity with stress in different magnetic field environments

memory signal will change more obviously. [22] shows that the environmental magnetic field plays an important role as the excitation magnetic field in the mechano-magnetic coupling. Under the same stress, the results detected in different excitation magnetic field environments are not the same. [23] explores the explanation of the magnetic memory effect mechanism of ferromagnetic materials under tensile load through the theory of dislocation and magnetic domain interaction. However, the specific influence mechanism of the environmental excitation magnetic field on the magnetic memory signal is still unclear [24].

2.2 Relationship between stress and relative permeability

Permeability is a physical quantity that characterizes the magnetic properties of a magnetic medium. In ferromagnetism, the relative permeability μ is defined as [25]:

$$\mu = \chi + 1 = \frac{M}{H} + 1 \tag{8}$$

In the equation, χ is the magnetic susceptibility, M is the magnetization, and H is the ambient magnetic field. From the relationship between the stress and the magnetization in the Eq. (7) and the relationship between the relative permeability and the magnetization in the Eq. (8). Under the excitation of different environmental magnetic fields, the relationship between the relative permeability μ and the stress σ can be obtained.

When the ferromagnetic material is damaged, the magnetic permeability of the damaged part is smaller than that of the non-damaged part, which causes the magnetoresistance of the defect to increase, the magnetic field will be distorted, and the magnetic field of the damaged part will be distorted. Equation (8) represents the relationship between magnetic permeability, magnetization and magnetic field strength. When the material is under tension, the stress will cause the magnetoelastic energy to change, causing the magnetic domain wall to move and bend, and the magnetization direction of the magnetic domain will turn to the direction of the stress to offset the increase in stress energy, and the overall magnetization of the material will become larger, until the stress increases to a certain level, the pinning effect inside the material will continue to increase, and the increase in magnetization will gradually weaken. Under the action of stress, with the generation of magnetic domain wall displacement and magnetic domain rotation, the demagnetizing field of the material will continue to increase, which will cause the magnetization to continue to decrease, and then leading to the change of permeability.

Use weak magnetic fields of different strengths as the excitation magnetic field to simulate the mechanical and magnetic coupling of the steel cable, and import the relative permeability corresponding to different tensile stresses under different magnetic field environments into the simulation model to calculate the mechanical and magnetic coupling, so as to determine the different magnetic fields. The relative magnetic permeability values corresponding to the environment and different stresses are used to establish the basis of force-magnetic coupling simulation.

3 Ansys simulation analysis

3.1 Simulation process and model establishment

This article uses ANSYS workbench magnetostatics module and the corresponding stress permeability change relationship of formula (8) to simulate the force-magnetic coupling. Under the action of tensile force, explore the law of the change of magnetic memory signals in the normal and tangential directions of the material surface under different environmental magnetic fields. The simulation flow chart of force-magnetic coupling is shown in Fig. 3:

The force-magnetic coupling simulation model is composed of magnet, armature, 60 steel (steel for steel wire rope), and air domain. To simulate the geomagnetic field and weak magnetic field environment by changing the parameters of permanent magnet, the statics module of ANSYS software is used to solve the equivalent stress. Combined with the stress permeability relationship of Eq. (8), the permeability of the material is defined in the magnetostatics module to realize the coupled simulation of statics and magnetostatics. Figure 4 shows the three-dimensional view of the cylindrical 60 steel specimen, the overall size and the collection path range of the magnetic memory signal. The middle part of the specimen is a penetration defect with a depth of 2.5 mm and a width of 2 mm. The environmental magnetic field simulation model and the magnetic field distribution represented by the magnetic field lines in the model are shown in Fig. 5. Figure 6 shows the force-magnetic coupling simulation model. The middle part of the model is a simulated cylindrical 60 steel specimen, the change of color from green to yellow represents the change of magnetic induction intensity from large to small, In this paper, the mechanical and magnetic coupling simulation of 60 steel with different defects set up two different magnetic field environments: geomagnetic field, weak magnetic excitation magnetic field (100 A/m), and three different tensile forces of 10 kN, 15 kN, and 20 kN. From the mechanical properties of 60 steel in
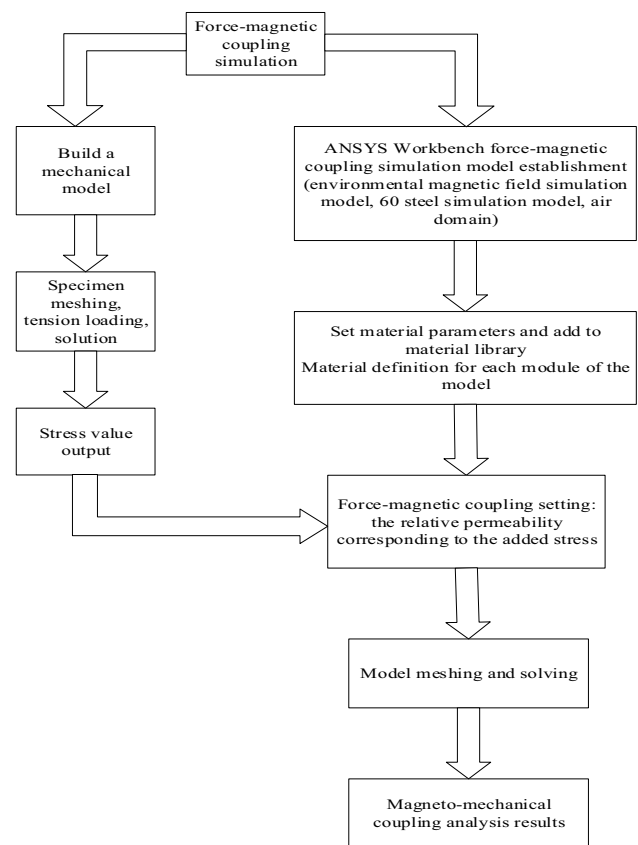

Fig. 3 Simulation flow chart of force-magnetic coupling

Table 1, it can be seen that the loaded stress range in this paper is within its elastic deformation range.

3.2 Simulation results and analysis

3.2.1 The magnetic memory signal changes under different weak magnetic fields under the action of pulling force

Figures 7, 9 and Figs. 8, 10 respectively show the normal and tangential components of the magnetic memory signal of the longitudinal crack and the transverse crack under different tensile forces in different magnetic field environments. In order to ensure the consistency of the magnetic memory signal detection between the simulation and the actual test, the acquisition path of the magnetic memory signal in the ANSYS Workbench simulation is set on the surface of the defect side of the specimen, the path length is set to 100 mm, and the defect center is located in the midpoint of the detection path.

The curve change trend shows: under the action of the environmental magnetic field, the difference between the peak and the trough of the magnetic memory signal gradually increases with the increase of the tensile force,
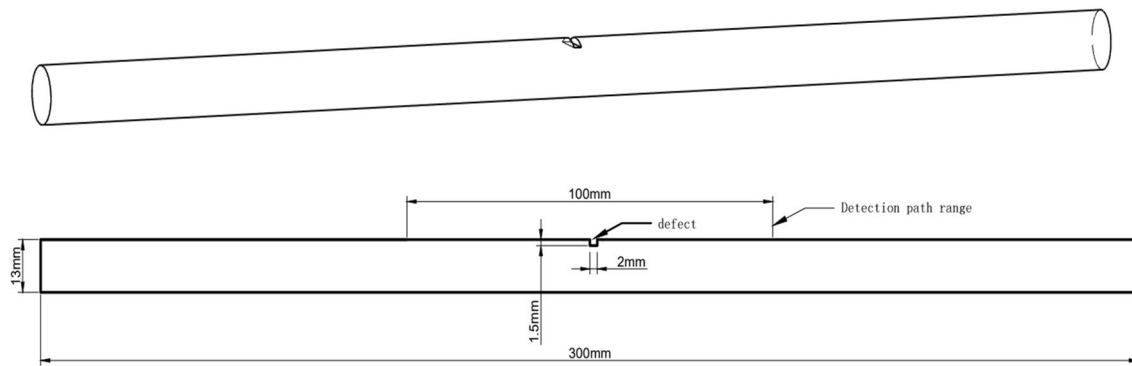
Fig. 4 Three-dimensional view and overall size of cylindrical 60 steel specimen and detection path range of magnetic memory signal
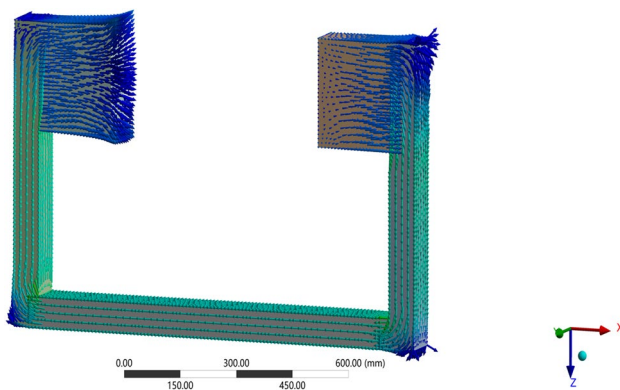

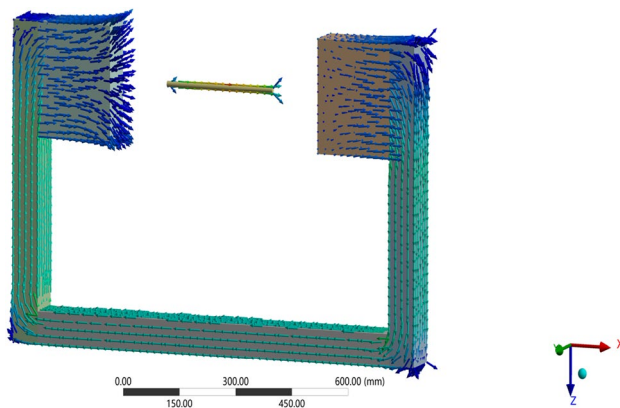**Fig. 5** Simulation model of environmental magnetic field

Fig. 6 Force-magnetic coupling simulation model

Table 1 Material properties and mechanical properties of 60 steel

Material	Modulus of elasticity /MPa	Poisson's ratio	Density / (kg/m^3)	The yield strength (σs)/MPa	Tensile strength (σb)/ MPa
60 carbon structural steel	210,000	0.3	7800	400	675

the continuous increase of the ambient magnetic field strength around the specimen, the leakage magnetic field strength also continues to increase. Because the magnetic permeability of the damaged part of the material is relatively smaller, it is more conducive to the formation of the distorted magnetic field. Thus the leakage magnetic field generated is also the largest, the magnetic memory signal changes of the normal component and the tangential component at the damaged part are more severe than other parts, the stress concentration points are further highlighted.

The normal component magnetic memory signal curve shows that the signal changes on both sides of the defect position show a steady upward trend, and the magnetic memory signal of the non-defective part of the tangential signal changes smoothly. Through the numerical analysis of Table 2, the comparison of the average value of the magnetic memory signal of the non-defect position under different tensile forces of the longitudinal crack and the transverse crack shows that with the increase of the tensile force, the average value of the magnetic memory signal of the normal component continues to decrease. Because under the action of tensile stress, the magnetic domain organization on the surface of the specimen gradually turns from a disordered state to an orderly and parallel to the direction of the external magnetic field, resulting in the average value of the normal component at the
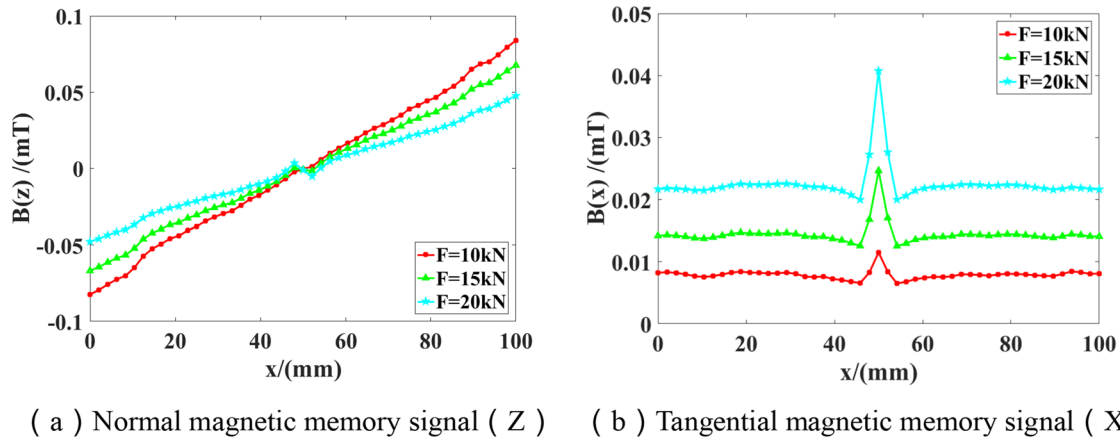
and the maximum abrupt change of the tangential signal defect is more obvious, resulting in divergent magnetic leakage on the surface of specimen damage. This is due to the directional or non-directional re-orientation of the magnetic domain organization in the ferromagnet under the action of stress, and then the leakage magnetic field is formed in the stress concentration position. With

（a）Normal magnetic memory signal（Z）   （b）Tangential magnetic memory signal（X）

Fig. 7 Magnetic memory signal changes in geomagnetic field under different tensile forces of longitudinal cracks. **a** Normal magnetic memory signal (Z). **b** Tangential magnetic memory signal (X)

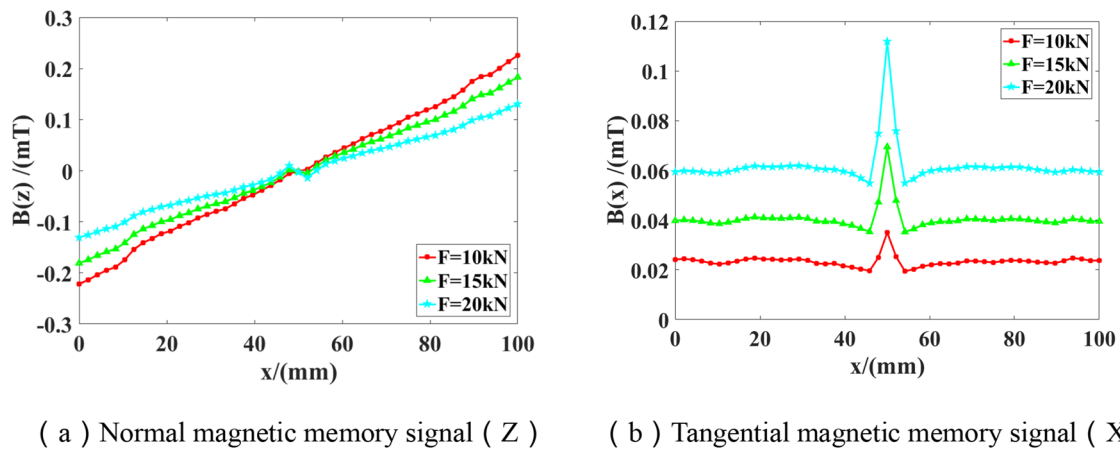（a）Normal magnetic memory signal（Z）   （b）Tangential magnetic memory signal（X）

Fig. 8 Magnetic memory signal changes in the excitation field under different tensile forces of longitudinal cracks. **a** Normal magnetic memory signal (Z). **b**Tangential magnetic memory signal (X)
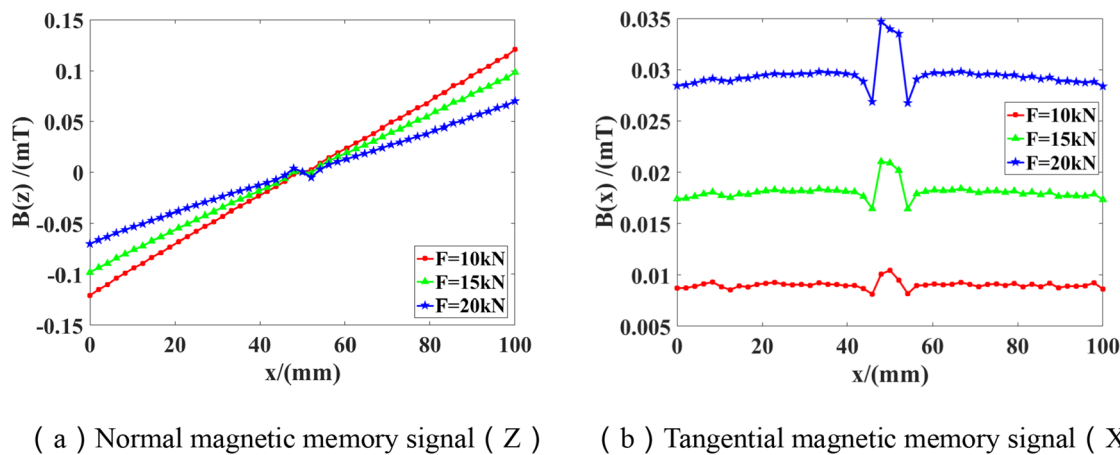

（a）Normal magnetic memory signal（Z）   （b）Tangential magnetic memory signal（X）

Fig. 9 Magnetic memory signal changes in geomagnetic environment under different tensile forces of transverse cracks. **a** Normal magnetic memory signal (Z). **b** Tangential magnetic memory signal (X)
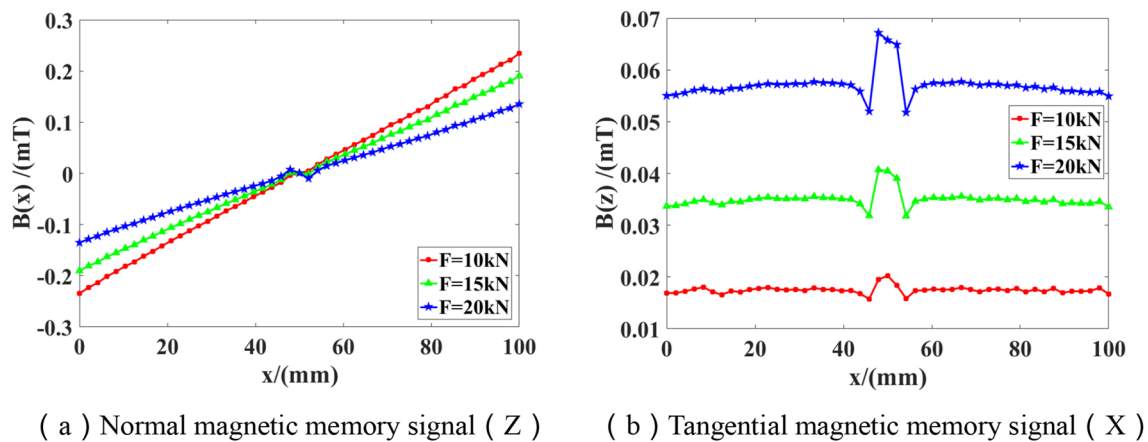
(a) Normal magnetic memory signal (Z)   (b) Tangential magnetic memory signal (X)

Fig. 10 Changes of magnetic memory signal in the magnetic field under the excitation of weak magnetic field under different tensile forces of transverse cracks. **a** Normal magnetic memory signal (Z). **a** Tangential magnetic memory signal (X)

non-defective position gradually decrease as the tensile force increases. Correspondingly, because the magnetic domain organization turns more toward the direction of the tangential component, the tangential component gradually increases under the action of increasing tensile stress. The change trend of the change curve of the longitudinal crack (Figs. 7 and 8) and the transverse crack (Figs. 9 and 10) of the magnetic memory signal indicates to a certain extent the change law of the microscopic magnetic domain structure under the coupling action of force and magnetic field.

It can be seen from Table 2 that the magnetic memory signal exhibits almost the same enhancement multiples under two different defects. Numerical analysis shows that the weak magnetic excitation magnetic field has a certain strengthening effect on the magnetic memory signal, and it also has a defect on the magnetic memory signal. The area and the non-defective area have the same degree of strengthening ability, so weak magnetic excitation will not affect the overall detection effect. It also helps eliminate interference in the environment, and is more conducive to highlighting and extracting magnetic memory signals, especially magnetic memory signals at defects in complex environments. Therefore, magnetic memory detection based on weak magnetic excitation will be more effective than traditional ground-based detection. Magnetic memory testing in a magnetic field environment can improve the problems that magnetic signal is relatively weak and not conducive to the highlighting of defects, which is more conducive to the location and quantitative analysis of the damage and stress concentration of the test piece, and improves the detection efficiency.

Through the simulation of different defect types, the magnetic memory signal results of Figs. 7, 8 and Figs. 9, 10 show that the change trend of the normal component

of the magnetic memory signal of different defect types is basically the same, but the tangential component has a sudden change at the defect. The obvious difference is that the abrupt change of the tangential component defect of the longitudinal crack presents a sharp peak, which is higher than that of the non-defect area. The sudden change of the tangential component defect of the transverse crack presents a sudden change first, then a gentle change, and then a sudden change, and the distance of the sudden change is longer than that of the longitudinal crack. This is determined by the different defect shapes of transverse cracks and longitudinal cracks. Therefore, the simulation analysis shows that the magnetic memory signal can not only locate the defect and the stress concentration, but also judge the damage shape of the test piece, which is convenient for identifying the type of defect. At the same time, the tangential component of the magnetic memory signal can better distinguish the shape of the defect than the normal component, and then judge the type of the defect.

Set the average value of the normal component magnetic induction intensity of the non-defective part of the magnetic memory signal on the surface of the test piece at different tensile forces of 10 kN, 15 kN, and 20 kN as B_{x1}, and the average value of the tangential component magnetic induction intensity as B_{y1}. The average value of the normal component magnetic induction intensity of the defect part is B_{x2}, and the average value of the tangential component magnetic induction intensity is B_{y2}. Set the strength of magnetic memory signal at the normal component non-defective part and the defective part under different magnetic field environments to Q1 and Q2, respectively, and the strength of the magnetic memory signal at the tangential component non-defective part and defective part to Q3 and Q4 respectively. Compare

Table 2 Numerical analysis of magnetic memory signals with different defects under stress in weak magnetic field and geomagnetic field

Defects and magnetic memory signal components			Geomagnetic field				Weak magnetic field excitation				Mean reinforcement ratio/A_Z	
			10 kN	15 kN	20 kN	Sum of averages/A_D	10 kN	15 kN	20 kN	Sum of averages/A_R		
Longitudinal crack defect	Normal component average (z) (mT)	Non-defective parts	0.0446	0.0358	0.025	0.1101	0.1199	0.0969	0.0684	0.2852	2.59	Q1
		Defective parts	0.0033	0.0021	0.0024	0.0078	0.0085	0.0059	0.0066	0.0209	2.679	Q2
	Mean value of tangential component(x) (mT)	Non-defective parts	0.0078	0.0141	0.0219	0.0438	0.0232	0.0397	0.0603	0.1232	2.813	Q3
		Defective parts	0.0083	0.0167	0.0271	0.0521	0.0249	0.0471	0.0745	0.1464	2.81	Q4
Transverse crack defect	Normal component average (Z) (mT)	Non-defective parts	0.0664	0.0535	0.0375	0.1574	0.1286	0.1037	0.0727	0.305	1.938	Q1
		Defective parts	0.0045	0.0029	0.003	0.0104	0.008	0.0057	0.0059	0.0204	1.962	Q2
	Mean value of tangential component(X) (mT)	Non-defective parts	0.009	0.018	0.0293	0.0563	0.0174	0.0348	0.0567	0.1089	1.934	Q3
		Defective parts	0.0093	0.019	0.0312	0.0595	0.0179	0.0368	0.0603	0.115	1.933	Q4

the degree of change of the magnetic memory signal under the excitation of a weak magnetic field.

As shown in Eqs. (9) and (10), the enhancement multiples of magnetic memory signals in the non-defective part of normal component and the defective part are set as Q1 and Q2 respectively under different magnetic field environments. As shown in Eqs. (11) and (12), the enhancement multiples of magnetic memory signals in the non-defective part of tangential component and the defective part are set as Q3 and Q4 respectively. The change degree of magnetic memory signal under weak magnetic field excitation was compared.

$$Q_1 = \frac{B_{(Geomagnetic\ field)x1}}{B_{(Weak\ magnetic\ excitation\ field)x1}} \tag{9}$$

$$Q_2 = \frac{B_{(Geomagnetic\ field)y1}}{B_{(Weak\ magnetic\ excitation\ field)y1}} \tag{10}$$

$$Q_3 = \frac{B_{(Geomagnetic\ field)x2}}{B_{(Weak\ magnetic\ excitation\ field)x2}} \tag{11}$$

$$Q_4 = \frac{B_{(Geomagnetic\ field)y2}}{B_{(Weak\ magnetic\ excitation\ field)y2}} \tag{12}$$

As shown in the Table 2, the mean value of magnetic memory signal values of non-defect parts and the mutation difference of defect parts extracted from specimens under different forces of 10kN, 15kN and 20kN. By averaging the values under different forces of geomagnetic field and weak magnetic field excitation environment, as shown in the table, the sum of the average values of different parts of the test piece under geomagnetic field and weak magnetic field is A_D and A_R, and the intensification multiple A_Z under geomagnetic field and weak magnetic field is obtained through Eq. (13).

$$A_Z = \frac{A_R}{A_D} \tag{13}$$

It can be seen from the A_Z value that in the weak magnetic excitation magnetic field environment, different defect types and non-defect parts in the specimen are strengthened with the same strength under the weak magnetic field. It can be seen that the weak magnetic excitation is to strengthen the overall magnetic memory signal of the specimen.
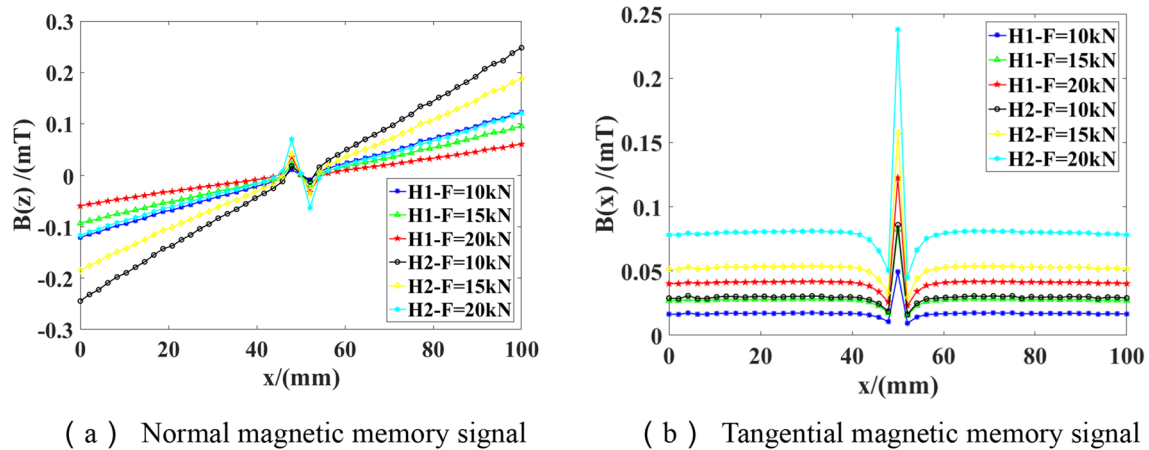
(a) Normal magnetic memory signal

(b) Tangential magnetic memory signal

Fig. 11 Magnetic memory signal changes under different pulling forces in excitation magnetic field environment. **a** Normal magnetic memory signal. **b** Tangential magnetic memory signal

3.2.2 The influence of a single weak magnetic excitation magnetic field on the magnetic memory signal under the action of tension

Figure 11 shows the change curve of the magnetic memory signal on the damaged part of the specimen under the excitation of a single weak magnetic field environment. Through the simulation analysis of the specimen with 2.5 mm defects, firstly, the mechanical and magnetic coupling simulation of the specimen under different tensile forces of 10 kN, 15 kN and 20 kN in the geomagnetic field, 100 A/m, 160 A/m different magnetic field environment is carried out, and the corresponding magnetic memory signal data is processed, and the data under the 160 A/m magnetic field environment is subtracted from the data under the geomagnetic field and the data under the 100 A/m magnetic field environment. Figure 11

shows the variation curves of magnetic memory signals in the acquisition path under the action of the same pulling force and different independent excitation magnetic fields. The greater the strength of the weak magnetic excitation magnetic field, the greater the distortion of the magnetic field caused by the changes in the magnetic domain organization caused by the stress at the specimen damage, which in turn will form a larger leakage magnetic field, and the more obvious the change of the magnetic memory signal. It can be seen from Fig. 11 that under the same pulling force, the application of different excitation magnetic fields has an obvious strengthening effect on the overall magnetic memory signal, especially the change of the magnetic memory signal at the defect site is more significant. This can be seen from the normal component and tangential component gradient map of the magnetic memory signal in Fig. 12. Under the same
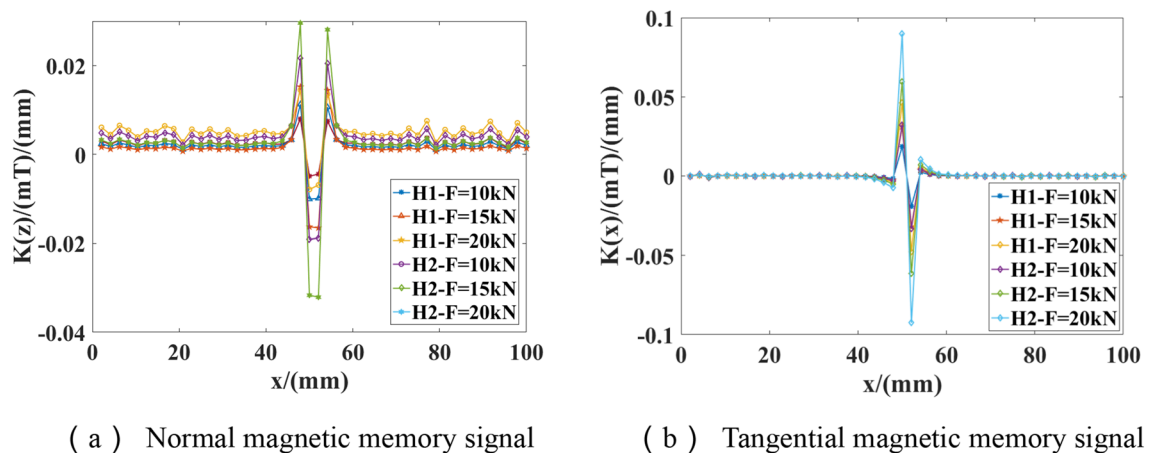

(a) Normal magnetic memory signal

(b) Tangential magnetic memory signal

Fig. 12 Magnetic memory signal gradient changes under different pulling forces in the excitation magnetic field environment. **a** Normal magnetic memory signal. **b** Tangential magnetic memory signal

tensile force at the damage site, the greater the strength of the single weak magnetic excitation magnetic field, the more obvious the gradient change of the magnetic memory signal. From the gradient map, we can see that the gradient change of the magnetic memory signal can better identify the defects of the specimen. In summary, the change of the magnetic memory signal under a single weak magnetic excitation magnetic field shows that the weak magnetic excitation magnetic field can strengthen the magnetic memory signal to a certain extent.

4 Test verification

The test uses permanent magnets as a weak magnetic field excitation source combined with an electronic universal testing machine to conduct a force-magnetic coupling test on a steel wire rope, and conduct a loading test by applying different loads to a wire rope with a diameter of 13 mm under the geomagnetic field and a weak magnetic excitation field to explore the changing law of the magnetic memory signal on the surface of the wire rope under the load of the environment and different tensile forces. Using the electronic universal testing machine as shown in Fig. 13, The load level of the testing machine is set to 0 kN, 10 kN, 20 kN, 30 kN, 40 kN, 50 kN, The magnetic field environments used in the experiment are the geomagnetic field and the weak magnetic excitation magnetic field. The weak magnetic excitation magnetic field is excited by a permanent magnet, and the magnetic field strength is set to 150A/m. The test equipment is shown in the figure:

By using the magnetic memory detector and its normal component detection probe as shown in Fig. 14 to perform point detection on the surface of the wire rope. Figure 15 shows the experimental wire rope and the detection points. According to the points shown in the figure, the same distance is taken for the defect and its upper and lower parts to extract the magnetic memory signal. and the datas of the detection result are processed, as shown


Fig. 14 Magnetic memory detector

in Fig. 16 shown is the change curve of the magnetic memory signal under different tension in the geomagnetic field environment. It can be seen from the graph that the magnetic memory signal curve of the non-defective part of the wire rope changes smoothly, showing a steady upward trend, and the defect part presents a trend of change in the shape of peaks and troughs. From the normal component graph, it can be seen that the geomagnetic field follows the tension the change of magnetic memory signal is relatively scattered, the change of magnetic memory signal at the defect is not concentrated, and it is relatively difficult to accurately judge the position of the defect. However, the change in the amplitude of the defect position displayed by the gradient transformation of the magnetic memory signal is more obvious than that of the non-defect position, but the gradient change of the magnetic field signal of the non-defect position is scattered, thus the relatively small defect cannot be accurately located and Identified.
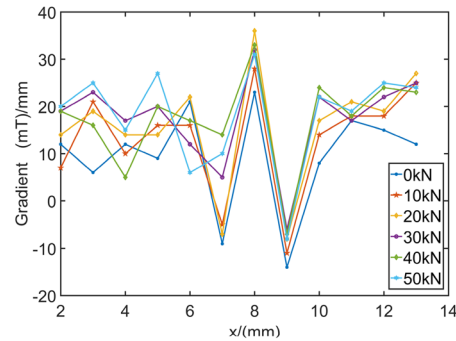
By applying a certain weak magnetic field excitation, the magnetic memory signal is strengthened to a certain extent. Figure 17 respectively shows the normal component of the magnetic memory signal and its gradient curve

Fig. 13 Force-magnetic coupling test equipment

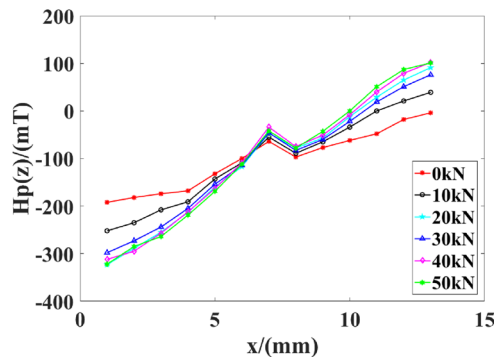

Fig. 15 Test wire rope and test point location
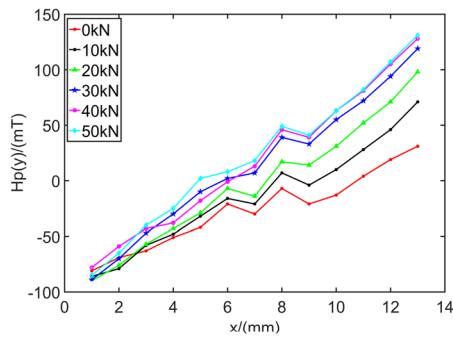
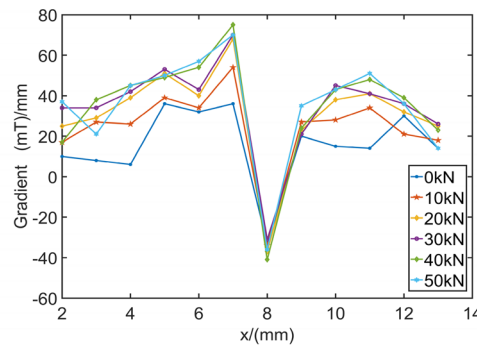（a）Normal component of magnetic memory signal

（b）Gradient curve of normal component of magnetic memory signal

Fig. 16 Variation curve of magnetic memory signal in geomagnetic field environment. **a** Normal component of magnetic memory signal. **b** Gradient curve of normal component of magnetic memory signal

（a）Normal component of magnetic memory signal

（b）Gradient curve of normal component of magnetic memory signal

Fig. 17 Change curve of magnetic memory signal in weak magnetic excitation magnetic field environment. **a** Normal component of magnetic memory signal. **b** Gradient curve of normal component of magnetic memory signal

under the weak magnetic excitation magnetic field environment. Compared with the geomagnetic field environment, the magnetic memory signal is more concentrated and the value of the overall signal is larger than that of the geomagnetic field. It can be seen that the weak magnetic excitation magnetic field has strengthened the magnetic memory signal to a certain extent, which is a good verification in the simulation. The conclusion that the magnetic memory signal can be strengthened in a weak magnetic field environment. It can be seen from the curve change that the magnetic memory signal is more concentrated, indicating that the weak magnetic excitation magnetic field strengthens the magnetic memory signal of the wire rope while suppressing the environmental stray signal around the specimen to a certain extent, which is beneficial to highlight the specimen itself, especially magnetic memory signal at the defect.

5 Conclusion

This paper discusses the J–A model theory based on weak magnetic excitation as the theoretical basis, and discusses the damage detection of steel wire ropes through ANSYS simulation analysis and tensile experiments. The conclusions are as follows: The improved J–A model can be well applied to simulation and experimental analysis under weak magnetic field excitation. The weak magnetic excitation has a certain strengthening effect on the magnetic memory signal under the force-magnetic coupling, and can restrain the interference in the geomagnetic field environment to a certain extent, which is beneficial to improve the relatively weak magnetic memory signal based on the geomagnetic field environment and improve the detection effect.

According to the change of the magnetic memory signal curve, the type of damage can be further analyzed and judged. The experimental results show that the metal magnetic memory under weak magnetic excitation can be better applied to the detection of wire rope damage, and the detection effect can be improved. It can be better applied to the damage detection of ferromagnetic materials in complex environments. This study is based on the research analysis of different types of defects to detect the damage site. Further, in practical engineering applications, it is also of great significance to study and realize the quantitative detection of different damage sizes of materials, and it will help to form a complete damage research system.

Declarations

Conflict of interest The authors declare that they have no conflict of interest.

Ethical approval This article does not contain any studies with human participants or animals performed by any of the authors.

References

1. Xu B, Jin GF, Guan Y (2018) Finite element analysis of magnetic memory signal characteristics near cracks. Nondestruct Test 042(006):25–26
2. Bao S, Jin P, Zhao Z, Fu M (2020) A review of the metal magnetic memory method. J Nondestr Eval 39(1):11
3. Lu BB, Wang HD, Dong LH, Zhao YC, Wang HP (2021) The application status and development prospects of metal magnetic memory fatigue damage detection. Mater Rev 35(07):7139–7144
4. Ren JL, Lin JM (2008) Electromagnetic nondestructive testing. Science Press, Beijing
5. Liu ZF, Fei ZY, Huang HH, Qian ZC (2018) Research on the strengthening mechanism of excitation magnetic field on the force-magnetic coupling effect. China Mech Eng 29(9):1108–1114
6. Bao S, Lou HJ, Fu ML, Gu YB (2017) Correlation of stress concentration degree with residual magnetic field of ferromagnetic steel subjected to tensile stress. Nondestruct Test Eval 32(3):255–268
7. Vlasov VT, Dubov A (2019) Physical bases of the metal magnetic memory method, 2nd edn. Spektr, Moscow
8. Liu B, Fu P, Li R, He P, Dong S (2019) Influence of crack size on stress evaluation of ferromagnetic low alloy steel with metal magnetic memory technology. Materials 12(24):4028
9. Huang H, Cheng Y, Qian Z, Gang H, Liu Z (2016) Magnetic memory signals variation induced by applied magnetic field and static tensile stress in ferromagnetic steel. J Magn Magn Mater 416:213–219
10. Zhang WM, Qiu ZC, Yu X, Sun HB (2015) Feasibility analysis of using enhanced magnetic excitation field to improve the sensitivity of magnetic memory detection. China Mech Eng 26(24):3375–3378
11. Chen HT (2016) Research on several key issues of magnetic memory testing of ferromagnetic materials. Nanchang Hang Kong University, Nanchang
12. Duan ZX, Ren SK, Zhao ZY, Zu RL, Fan QQ (2017) The influence of environmental magnetic field on magnetic memory signal. Fail Anal Prev 12(01):13–18+32
13. Fan QQ, Ren SK, Ren XZ, Xu Y, Duan ZX (2019) Experimental study on the influence of external magnetic field on the magnetic effect of Q235 steel. China Test 45(06):46–53
14. Wang H, Dong L, Wang H, Ma G, Zhao Y (2021) Effect of tensile stress on metal magnetic memory signals during on-line measurement in ferromagnetic steel. NDT&E Int 117:102378
15. Su SQ et al. New progress and key issues in metal magnetic memory testing technology. Chin J Eng Sci 42(12):16
16. Kaminski DA, Jiles DC, Biner SB, Sablik MJ (1992) Angular dependence of the magnetic properties of polycrystalline iron under the action of uniaxial stress. J Magn Magn Mater 1(104–107):328–384
17. Ren SK, Ren XZ, Duan ZX, Fu YW (2019) Studies on influences of initial magnetization state on metal magnetic memory signal. NDT&E Int 103:77–83
18. Jiles DC, Atherton DL (1984) Theory of magnetization process in ferromagnets and its application to the magnetomechanical effect. J Phys D 17(6):1265–1281
19. Jiles DC (1995) Theory of the magnetomechanical effect. J Phys D 28(8):1537–1546
20. Kuruzar ME, Cullity BD (1971) The magnetostriction of iron under tensile and compressive stress. Int J Magn 1(4):323
21. Tang YL (2016) Research on defect detection technology based on magnetic memory
22. Yang E, Li L (2005) Magnetization changes induced by low cycle fatigue both in the geomagnetic field and the magnetic-free environment. Nondestructive evaulation for health monitoring and diagnostics. International Society for Optics and Photonics, SanDiega, pp 373–380
23. Shi CL, Dong SY, Xu BS, He P (2010) Metal magnetic memory effect caused by static tension load in a case-hardened steel. J Magn Magn Mater 322(4):413–416
24. Zhong LQ, Li LM, Chen X (2010) Magnetic signals of stress concentration detected in different magnetic environment. Nondestruct Test Eval 25(2):161–168
25. Yan M, Peng XL (2019) Fundamentals of magnetism and magnetic materials. Zhejiang University Press, Hangzhou

Publisher's Note Springer Nature remains neutral with regard to jurisdictional claims in published maps and institutional affiliations.